

Interplay of polymer crystallization and
liquid-liquid demixing in solutions studied by
lattice-model theory and simulations

Wenbing Hu¹, Daan Frenkel¹, Mark Miller¹, Vincent B. F. Mathot²

¹FOM Institute for Atomic and Molecular Physics,
Kruislaan 407, 1098 SJ Amsterdam, The Netherlands

²DSM Research, P. O. Box 18 Geleen, The Netherlands

February 7, 2020

Abstract

We report dynamic Monte Carlo simulations and statistical thermodynamic theories of a lattice-polymer model, in which polymer crystallization and liquid-liquid demixing of semiflexible homopolymer solutions were investigated simultaneously. In our simulations, the equilibrium phase transition temperature was approached by the onset of phase transitions on cooling, when an introduced substrate greatly decreased the kinetic delay caused by the homogeneous nucleation. The simulation results about the phase transition temperatures and their shift due to the interplay of phase transitions showed good agreement with the predictions of mean-field theories. In addition, upon cooling through the monotectic triple point in a concentrated solution, our simulation found that liquid-liquid demixing is kinetically favored over crystallization in the competition of homogeneous nucleations.

1 Introduction

Lattice models of polymer solutions are widely used because of their simplicity and computational convenience. [1–8] When modeling a polymer solution, the polymer chain occupies consecutive sites on the lattice, each site corresponding to the size of one chain unit, while the remaining sites correspond to solvent.

The use of lattice models for polymer solutions dates back to the work of Meyer [1]. Flory [2] and Huggins [3] showed how, using a mean-field approximation, the lattice model yielded a powerful tool to predict the solution properties of flexible [9–11] and semi-flexible [7] polymers. Various refinements to the Flory-Huggins (F-H) model have been proposed by a number of authors (see, e.g. Refs. [4] to [6]). FH-style models can account for liquid-liquid (L-L) phase separations with an upper critical solution temperature (UCST) driven by the site-to-site mixing pair interactions in polymer solutions - however, they are ill suited to describe polymer crystallization, i.e. liquid-solid (L-S) phase transitions. As was shown in Ref. [8], this limitation is not due to any intrinsic drawback of the lattice model as such, but to the nature of the mean-field approximation used in the F-H theory, since the driving forces for polymer crystallization, i.e. the compact packing tendency and chain inflexibility, can be expressed in bond-to-bond anisotropic pair interactions. Clearly, in real polymer solutions, both crystallization and phase separation can occur on cooling. While lattice

models for polymer solutions can account for both types of phase transitions, most theoretical and simulation studies have focused on one transition or the other, and little attention has been paid to their interplay. Such interplay may change the pathway of a phase transition [12, 13] and hence determines the complex structure-property relationships of crystallizable polymer mixtures, stimulating much experimental research dating back to Richards. [14]

When L-S phase transition curve intersects L-L coexistence curve, both curves are terminated at the crossing point as a result of thermodynamic competition between two kinds of phase transition. At the crossing point, the fluid phase may phase-separate into a dilute solution and a dense crystalline phase, as depicted in Fig.1. This combination of L-L demixing and crystallization is often referred to as "monotectic" behavior and has been observed in many experiments. [10, 15, 16] Special attention has been focused on the crossing point (monotectic triple point), near which the kinetic competition between L-L demixing and crystallization on cooling is an important issue for sol-gel transition and membrane preparation. [17–19] Under these conditions, L-L phase separation is expected to occur before crystallization. [20] Hence, the modulated concentration structures produced during the early stage of L-L demixing may be frozen in by subsequent crystallization. [21] This suggests a practical way to control the metastable morphology of polymer gels and membranes through thermally induced

processes. A prediction of phase diagrams like Fig. 1 is of essential importance in designing this kind of process.

In this paper, we study the interplay of polymer crystallization and L-L demixing through current lattice theories and dynamic Monte Carlo simulations. In particular, we notice the shift of the crystallization and L-L demixing curves on the phase diagrams due to this interplay.

The remainder of this paper is organized as follows: after an introductory description of the simulation techniques, we compare the simulation results with the relevant theoretical predictions for the L-S phase transition curve in subsection 1, and the L-L phase separation curve in subsection 2. In both cases, the interplay of phase transitions is avoided. Then, we discuss the competition between these phase transitions on cooling, considering thermodynamic and kinetic aspects separately.

2 Simulation Techniques

In our Monte Carlo simulations, we used the single-site-jumping model with local sliding diffusions [22] to model the evolution of self- and mutually-avoiding polymers in a lattice box with periodic boundary conditions. In a cubic lattice, jumping was permitted along either the grid lines or the diagonals, so the coordination number of each site includes all the neighboring sites along the grid lines and the diagonals, and is $9+8+9 = 26$. The validity of this model has been verified by reproducing the size- and

time-scaling laws of short-chain polymers in the molten state. [23]

In a typical system, we considered a number of polymer chains, each consisting of 32 units. The polymers reside in a cubic box with 32^3 lattice sites. The polymer concentration was varied by changing the number of polymers in the simulation box. The Monte Carlo sampling was performed using the Metropolis method. Three energetic parameters were used to model the intra- and inter-molecular interactions of the polymers. The first parameter E_c measures the energy penalty associated with having two non-collinear consecutive bonds (a "kink") along the chain, reflecting the rigidity of chains. The second parameter E_p measures the energy difference between a pair of non-parallel and parallel polymer bonds in non-bonded adjacent positions, reflecting the compact packing tendency of chain-like molecules in crystallization. Finally, the parameter B describes the polymer-solvent site-to-site mixing tendency. B is equal to the energetic loss of a polymer-solvent contact compared to an average over a polymer-polymer contact and a solvent-solvent contact. The total change in potential energy associated with a Monte Carlo trial move is

$$\begin{aligned}\frac{\Delta E}{k_B T} &= \frac{E_c \Delta c + E_p \Delta p + B \Delta m}{k_B T} \\ &= (\Delta c + \Delta p \frac{E_p}{E_c} + \Delta m \frac{B}{E_c}) \frac{E_c}{k_B T},\end{aligned}\tag{1}$$

where Δc , Δp and Δm denote the net changes in the number of kinks (Δc),

the number of non-parallel packing pairs (Δp) and the number of polymer-solvent contacts (Δm), k_B is the Boltzmann constant and T temperature. As shown in Eq. 1, three dimensionless parameters control the acceptance probability of Monte Carlo trial moves: E_p/E_c , the term that reflects the molecular driving force for crystallization, B/E_c , the term that reflects the molecular driving force for L-L demixing, and $E_c/(k_B T)$, which is a measure for the system temperature. In our simulations, $E_c \gg E_p$ corresponds to rigid chains, while setting E_c to zero simulates flexible chains. Therefore, we chose $E_p/E_c = 1$ to study the crystallization of semiflexible chains. A proper choosing on the value of B/E_c to study the L-L demixing will be discussed in the next section. We increased the value of $E_c/(k_B T)$ from zero in steps of 0.002. At each step, the total number of trial moves was 500 MC cycles, where one Monte Carlo cycle (MC cycle) is defined as one trial move of each chain unit on average. The first 400 MC cycles at each temperature were discarded for equilibration, after which samples were taken once per MC cycle and averaged. This process corresponds to a slow cooling of the sample system.

We approach the equilibrium phase-transition temperature through a dynamic cooling process. As in the practical experiments, the onset temperature of phase transition on stepwise cooling reflects the position of the L-S or L-L coexistence curves at the preset concentration. However, taking temperature steps of equal size may lead to overshooting of the phase tran-

sition temperature due to a kinetic barrier for homogeneous nucleation. This is particularly true in dilute solution and with a limited size of simulation box. In order to approach the equilibrium phase-transition point, this kinetic effect should be diminished as far as possible. Therefore, we introduced one layer of terraced substrate fixed with extended chains, as demonstrated in Fig. 2A. For generating crystallization on cooling, layer-by-layer crystal growth can directly happen on a large-size terraced substrate in avoidance of homogeneous nucleation. This looks mostly like a self-seeded heterogeneous nucleation. Furthermore, a smart cooling process was applied to enhance the sharpness of phase transitions and make their onset obvious. In this cooling process, the recorded data in each period (500 MC cycles) of step was compared with the previous one, and if it showed the phase transition tendency, the value of $E_c/(k_B T)$ would not jump to the next until the recorded data of the subsequent periods showed a reverse tendency produced in thermal fluctuations.

On cooling, the ordering status of the sample system can be traced by the Flory "disorder" parameter, defined as the mean fraction of non-collinear connections of two consecutive bonds along the chains. For the present model, where 24 out of 25 connections are non-collinear, the high-temperature limit of the disorder parameter is 0.96. Meanwhile, the mixing status of the sample system can be traced by the value of a "mixing" parameter, defined as the mean fraction of the coordinate sites around each

chain unit that is occupied by solvent. This parameter allows us to trace the demixing transition on cooling within the whole concentration range. In this paper, we report the onsets of phase transitions averaged over five individual cooling processes with the same settings but with different seeds of random-number generation.

As demonstrated in Fig. 2B, introducing a terraced substrate can significantly decrease the kinetic delay on cooling for polymer crystallization in a solution near the dilute end. The onset of crystallization induced by the terraced substrate becomes insensitive to the number of steps on the substrate when this number is more than 8, see Fig. 2C. This implies that when the number of steps is 32 the pretransitional absorption of chains on the substrate has negligible effect on the concentration. A significant finite-size effect of the simulation box on the onset of crystallization has been observed for the sample system at dilute concentrations. This effect can be mainly attributed to the volume dependence of the homogeneous nucleation rate, and be eliminated by the introduction of a terraced substrate that induces heterogeneous nucleation, see Fig. 2D.

In the following sections, we first set B/E_c equal to zero, corresponding to the case where only crystallization occurs on cooling. Next, we set E_p/E_c to zero, while making B/E_c large enough, to study only L-L demixing on cooling. Finally both parameters were set to non-zero values, in order to study the interplay of polymer crystallization and L-L demixing in solu-

tions.

3 Results and Discussion

3.1 Crystallization without liquid-liquid demixing

When we set $B/E_c = 0$ and $E_p/E_c = 1$, only the driving forces for polymer crystallization are switched on. The onset temperature of crystallization induced by the terraced substrate can be regarded as a good approximation to the equilibrium melting point and can be compared to the predictions of mean-field theory.

In Ref. [8], the partition function of the mixed and disordered state of polymer solution was calculated as

$$Z = \left(\frac{n}{n_1}\right)^{n_1} \left(\frac{n}{n_2}\right)^{n_2} \left(\frac{q}{2}\right)^{n_2} z_c^{(r-2)n_2} e^{(1-r)n_2} z_p^{(r-1)n_2} z_l^{rn_2}, \quad (2)$$

in which

$$z_c = 1 + (q - 2) \exp\left(-\frac{E_c}{k_B T}\right),$$

$$z_p = \exp\left[-\frac{q-2}{2}(2 - \frac{rn_2}{n} - \frac{4}{q}) \frac{rn_2}{n} \frac{E_p}{k_B T}\right],$$

$$z_l = \exp\left(-\frac{n_1}{n} \frac{q_{eff} B}{k_B T}\right),$$

n_1 denotes the number of sites occupied by the solvent, n_2 the number of chains, each having r units, $n = n_1 + rn_2$, q is the coordination number, and q_{eff} the effective q for the mixing interactions.

Eq. 2 was derived by treating the demixed and fully ordered state

of polymer solution as the ground state, which has the partition function equal to one. So, the equilibrium temperature of the disorder-order phase transition can be calculated from the equation $Z = 1$ by iteration. However, the theoretical results shown in the dashed curve of Fig. 3 give a poor prediction of the equilibrium melting points except at high concentration, in comparison with the simulation results on cooling either with a terraced substrate or under the absence of substrate. This dashed curve seems to fit better to the simulation results under the absence of substrate than to those with a terraced substrate, but this is a less meaningful comparison on account of the significant kinetic effect of phase transitions on cooling under the absence of substrate.

In fact, the large deviation on dilution can be attributed to a term missing from the estimated contribution of E_p in Eq. 2. In Ref. [8], we calculated the probability of finding a bond occupying the parallel position neighboring to an arbitrary bond as $4\phi/q$, where $\phi = rn_2/n$ is the polymer volume fraction. The probability of non-parallel occupation of this bond position was calculated by the subtraction of $4\phi/q$ from the probabilities of both double occupation and single occupation, but excluding the probability of zero occupation. However, with a reference of the fully phase-separated and ordered ground state, zero occupation is energetically equivalent to a kind of non-parallel packing state, whose contribution will become significant on dilution. Therefore, the correct probability of non-parallel occupa-

tion should be $1 - 4\phi/q$ and the E_p contribution in Eq. 2 can be improved to give a new version of Eq. 2

$$Z = \left(\frac{n}{n_1}\right)^{n_1} \left(\frac{n}{n_2}\right)^{n_2} \left(\frac{q}{2}\right)^{n_2} z_c^{(r-2)n_2} e^{(1-r)n_2} z_p^{(r-1)n_2} z_l^{rn_2}, \quad (3)$$

in which

$$\begin{aligned} z_c &= 1 + (q-2)\exp\left(-\frac{E_c}{k_B T}\right), \\ z_p &= \exp\left[-\frac{q-2}{2}\left(1 - \frac{4rn_2}{qn}\right)\frac{E_p}{k_B T}\right], \\ z_l &= \exp\left(-\frac{n_1}{n}\frac{q_{eff}B}{k_B T}\right). \end{aligned}$$

The predictions for the equilibrium melting point calculated from $Z = 1$ with Eq. 3 are shown in the solid curve of Fig. 3. Now, much better agreement can be observed between the theoretical predictions and the onsets of crystallization induced by a terraced substrate on cooling, especially in the dilute solutions.

Flory has derived the semi-empirical relationship between the melting point and the concentration of polymer in solutions, [24] as

$$\frac{1}{T_m} - \frac{1}{T_m^0} = \frac{k_B}{\Delta h_u} [1 - \phi - \frac{q_{eff}B}{k_B T_m} (1 - \phi)^2], \quad (4)$$

where T_m^0 is the bulk equilibrium melting point, Δh_u is the heat of fusion per monomer. The predictions of Eqn. 4 for the melting point depression upon dilution have been verified by several experimental measurements at both high and low concentrations [25, 26]. In Fig. 3, the reciprocal onset

temperatures of crystallization induced by a terraced substrate on cooling indeed follow a good linear relationship with polymer concentrations, as expected in Eq. 4 for the chains in an athermal solvent ($B = 0$).

3.2 Liquid-liquid demixing without crystallization

Even if we set both $B/E_c = 0$ and $E_p/E_c = 0$, a disorder-order phase transition may still occur on cooling in the short chain system with high polymer concentrations. [8, 27] This transition is not, strictly speaking, a freezing transition but rather an isotropic-nematic phase transition: it is induced by the anisotropic excluded volume interactions between polymer chains, as the chain rigidity is increased with decreasing temperature. [7, 28] This transition has recently been studied extensively by Weber et al. [29]

If we increase the value of B/E_c while keeping E_p/E_c equal to zero, we should reach a point above which L-L demixing occurs prior to the isotropic-nematic phase transition on cooling. We focused our attention on the L-L demixing with the values of B/E_c beyond that critical point, and kept track of the "mixing" parameter during a smart cooling. As the same as in the previous section, the onset temperature of L-L demixing induced by a terraced substrate on cooling should be a good approximation to the equilibrium phase separation temperature. A tentative binodal curve can thus be obtained in simulations to compare with the predictions of mean-field theories.

Figure 4 shows the binodal curves for the sample systems with $E_p/E_c = 0$ and $B/E_c = 0.25$. The binodal curve estimated on the basis of F-H expression for the mixing free energy change (see Eq. 5), shows a small but constant deviation from the simulation results. As a matter of fact, Eq. 5 can be reproduced from Eq. 3 when setting $E_p = 0$ and $q_{\text{eff}} = q - 2$.

$$\begin{aligned} \frac{\Delta F_{\text{mix}}}{k_B T} = & (1 - \phi) \ln(1 - \phi) + \frac{\phi}{r} \ln(\phi) \\ & + \phi(1 - \phi) \frac{(q - 2)B}{k_B T}. \end{aligned} \quad (5)$$

The lattice-cluster theory has been found to provide a much better fit to computer simulation results about the binodal curve when its second-order expansion is employed. [30] To second order, the mixing free energy change per lattice site is [6]

$$\begin{aligned} \frac{\Delta F_{\text{mix}}}{k_B T} = & (1 - \phi) \ln(1 - \phi) + \frac{\phi}{r} \ln(\phi) \\ & - \frac{1}{2} q \epsilon \phi^2 + C_0 + C_1 \phi + C_2 \phi^2, \end{aligned} \quad (6)$$

where C_0 , C_1 and C_2 were chosen as the same as in Ref. [6], and $\epsilon = 2B/(k_B T)$. From moderate to high polymer concentrations, the binodal curve predicted by the lattice cluster theory (dashed curve in Fig. 4) indeed yields better agreement than the F-H theory.

We note, however, that for very long polymer chains, the lattice cluster theory may predict more than one critical point. [31] Hence, the predictions

of this theory should be viewed with some caution. [32]

3.3 Interplay between crystallization and liquid-liquid demixing

3.3.1 Thermodynamic competition

We have exploited the fact that the model with $B/E_c = 0$ and $E_p/E_c = 1$ yields only crystallization on cooling, while the model with $E_p/E_c = 0$ and $B/E_c = 0.25$ yields only L-L demixing on cooling. By going from the models for either $E_p/E_c = 0$ or $B/E_c = 0$ to one where both parameters are non-zero, we can "tune" the interplay between crystallization and L-L demixing. According to Eq. 3, we expect that a positive value of B/E_c should increase the stability of any dense phase, in particular the crystal; on the other hand, a positive value of E_p/E_c should also raise the L-L demixing temperature. In fact, this is precisely the behavior observed in Fig. 5, where the L-L demixing curve of the sample system with $B/E_c = 0.25$ shifts up when the value of E_p/E_c changes from zero to one. A serious values of B/E_c changing from negative to positive make the melting point curves changing from decreasing to increasing on dilution. The comparisons between Fig. 5A (the predictions from Eq. 3) and B (the simulation results) show good agreements under the same scales of axes. The simulations can furthermore show the crystallization with prior phase separation on cooling. However, a second common crossing point for the simulation L-S transition curves is found at the concentration of 0.73 besides the expected value of 1.00. The

occurrence of this point is not related with the introduction of a terraced substrate, since it also exists in the onsets of crystallization on cooling under the absence of substrate. [8] Rather, it may be a coupling result between two kinds of driving force respective to the different phase transitions, as has not been considered in current mean-field assumptions.

No matter with negative or positive values of B/E_c , the simulation results for the reciprocal melting temperatures still keep the good linear relationships with polymer concentrations, if without prior L-L phase separation (see Fig. 6). According to Eq. 4, the slopes obtained from linear regression give the values of $-q_{\text{eff}}B/\Delta h_u$ and the intercepts give the values of $E_c/\Delta h_u$. We further found that both the $-q_{\text{eff}}B/\Delta h_u$ vs. $B/E_c \times E_c/\Delta h_u$ curve and the $\Delta h_u/E_c$ vs. B/E_c curve have good linear relationships with the correlation coefficient 0.999 and 0.996 respectively. The slopes after linear regression give $q_{\text{eff}} = 54.0$ and $\Delta h_u = 41.0B + 13.0E_c$. The latter reflects a microscopic coupling between L-L demixing and polymer crystallization, consistent but not identical with the previous study. [8]

In Fig. 5B, the phase diagram with the setting parameter $E_p/E_c = 1$ and $B/E_c = 0.1$ follows the conventional expectations as demonstrated in Fig. 1, but that with the setting parameter $E_p/E_c = 1$ and $B/E_c = 0.25$ behaves quite differently. In a very poor solvent, the value of B/E_c is quite large, and the melting point can become increasing on dilution. Therefore on cooling, when L-L demixing occurs prior to crystallization, the subse-

quent crystallization should be at a temperature higher than the crossing point or the expected point without prior L-L demixing, since the crystallization can be induced by the dilute phase, which has higher melting point. However in Fig. 6, the crystallization temperatures with the setting parameter $E_p/E_c = 1$ and $B/E_c = 0.25$ and with prior L-L demixing, still show lower temperatures than the extrapolation of the linear regression curve calculated from the data points without prior demixing. This implies that the prior phase separation actually retards the crystallization on cooling. This may be attributed to the fact that the crystallization is still induced by the substrate covered with the concentrated phase that has a lower melting point. Here, the unusual phase diagram beyond the conventional expectation is caused by a high coordination number (26) in our simulations, which makes the slope of L-S transition curve sensitive to the value of B/E_c as demonstrated in Eq. 4 and negative before L-L coexistence curve shifting up over the L-S curve.

3.3.2 Kinetic competition

On cooling through the vicinity of the upper critical solution point on the L-L coexistence curve, the mechanism of phase separation should be a typical spinodal decomposition which shows no kinetic delay on cooling. When the monotectic triple point is quite close to this region, a cooling through this monotectic triple point where polymer crystallization and L-L demix-

ing are expected to have the same thermodynamic phase transition temperatures, will always show the L-L demixing prior to crystallization due to a significant kinetic delay for the nucleation-growth mechanism of crystallization. However, if the monotectic triple point is far away from the upper critical solution point, the mechanism of L-L demixing should also be a typical nucleation-growth like the crystallization, so a cooling through this triple point will show a kinetic competition between the homogeneous nucleations of two different kinds of phase transition.

In Fig. 5B, the monotectic triple point on the phase diagram with the setting parameter $E_p/E_c = 1$ and $B/E_c = 0.25$ is located at polymer volume fraction 0.8. This concentration is far away from the upper critical solution point. So, on cooling through this monotectic triple point and under the absence of substrate, the simulations should show a kinetic competition between two kinds of phase transitions. The results are shown in Fig. 7, where the L-L phase separation indeed needs less supercooling than crystallization, as first considered by Koningsveld. [20] Actually, this sequence in phase transitions reflects the sequence of their driving forces contributing to polymer cohesive energy, since crystallization from solution must have a demixing process at first.

4 Summary

Only switching on the driving force for crystallization, the onsets of phase transition on cooling with a terraced substrate show good agreement with the improved version of lattice statistical theory. On the other hand, only switching on the driving force for L-L demixing, the onsets of phase separation on cooling with a terraced substrate show good agreement with the F-H theory and the lattice cluster theory. When switching on driving forces for both phase transitions, their interplay still shows good agreement with the theoretical expectations. In simulations, the crystallization temperature with prior L-L demixing on cooling can be observed. Under the absence of substrate, cooling through the monotectic triple point shows the priority of L-L demixing over crystallization, even though that point locates in high concentrations.

Our effort here demonstrates that the mean-field lattice theory can give more comprehensive results about phase diagrams of polymer mixtures, and the computer simulations based on the lattice model can supply much more insights about the nature of polymer phase transitions in reality.

Acknowledgement This work was financially supported by DSM Company and the division of Chemical Science of the Netherlands Organization for Scientific Research (NWO). The work of the FOM Institute is part of the research program of FOM and is made possible by financial support from the NWO.

References

- [1] K.H. Meyer, Z. Phys. Chem. (Leipzig) B**44**, 383(1939).
- [2] P.J. Flory, J. Chem. Phys. **10**, 51(1942).
- [3] M.L. Huggins, Ann. N. Y. Acad. Sci. **43**, 1(1942).
- [4] R. Koningsveld, L.A. Kleijens, Macromol. **4**, 637(1971).
- [5] M.G. Bawendi, K.F. Freed, J. Chem. Phys. **88**, 2741(1988).
- [6] D. Buta, K.F. Freed, and I. Szleifer J. Chem. Phys. **112**, 6040(2000).
- [7] P.J. Flory, Proc. R. Soc. London, Ser. A **234**, 60(1956).
- [8] W.-B. Hu, J. Chem. Phys. **113**, 3901(2000).
- [9] E.A. Guggenheim, *Mixtures* (Clarendon, Oxford, 1952).
- [10] P.J. Flory, *Principles of Polymer Chemistry* (Cornell University Press, Ithaca, NY, 1953).
- [11] I. Prigogine, *The Molecular Theory of Solution* (Amsterdam, 1957).
- [12] P. R. ten Wolde, D. Frenkel, Science **277**, 1975(1997).
- [13] V. Talanquer, D. W. Oxtoby, J. Chem. Phys. **109**, 223(1998).
- [14] R.B. Richards, Trans. Faraday Soc. **42**, 10(1946).
- [15] L. Aerts, H. Berghmans, and R. Koningsveld, Makromol. Chem. **194**, 2697(1993).

[16] X.W. He, J. Herz, and J.M. Guenet, *Macromol.* **20**, 2003(1987).

[17] H.K. Lee, A.S. Myerson, and K. Levon, *Macromol.* **25**, 4002(1992) and ref. therein.

[18] J.M. Guenet, *Thermochimica Acta* **284**, 67(1996).

[19] H. Berghmans, R. De Cooman, J. De Rudder, and R. Koningsveld *Polymer* **39**, 4621(1998).

[20] R. Koningsveld, Ph.D. Thesis, University of Leiden, 1967.

[21] N. Inaba, K. Sato, S. Suzuki, T. Hashimoto *Macromol.* **19**, 1690(1986).

[22] W.-B. Hu, *J. Chem. Phys.* **109**, 3686(1998).

[23] W.-B. Hu, *J. Chem. Phys.* **115**, 4395(2001).

[24] P. J. Flory, *J. Chem. Phys.* **17**, 223(1949).

[25] L. Mandelkern, *Crystallization of Polymers* (McGraw-Hill Book Co., NY, 1964), p. 38.

[26] A. Prasad and L. Mandelkern, *Macromol.* **22**, 914(1989).

[27] A. Baumgaertner, *J. Chem. Phys.* **84**, 1905(1986).

[28] M. Dijkstra, D. Frenkel *Phys. Rev. E* **51**, 5891(1995).

[29] H. Weber, W. Paul and K. Binder, *Phys. Rev. E* **59**, 2168(1999).

[30] Q. Yan, H. Liu, and Y. Hu, *Macromol.* **29**, 4066(1996).

[31] B. Quinn, P.D. Gujrati, J. Chem. Phys. **110**, 1299(1999).

[32] K.F. Freed, J. Dudowicz, J. Chem. Phys. **110**, 1307(1999).

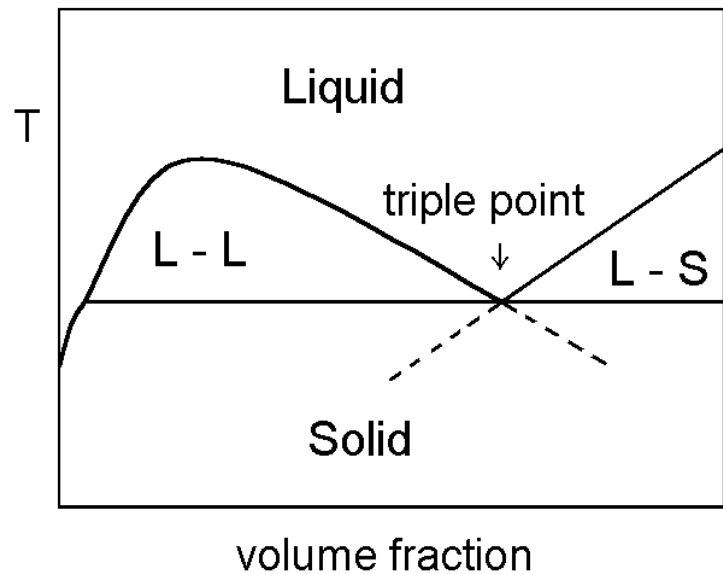


Figure 1: Schematic phase diagram of a binary mixture with a conventional monotectic triple point.

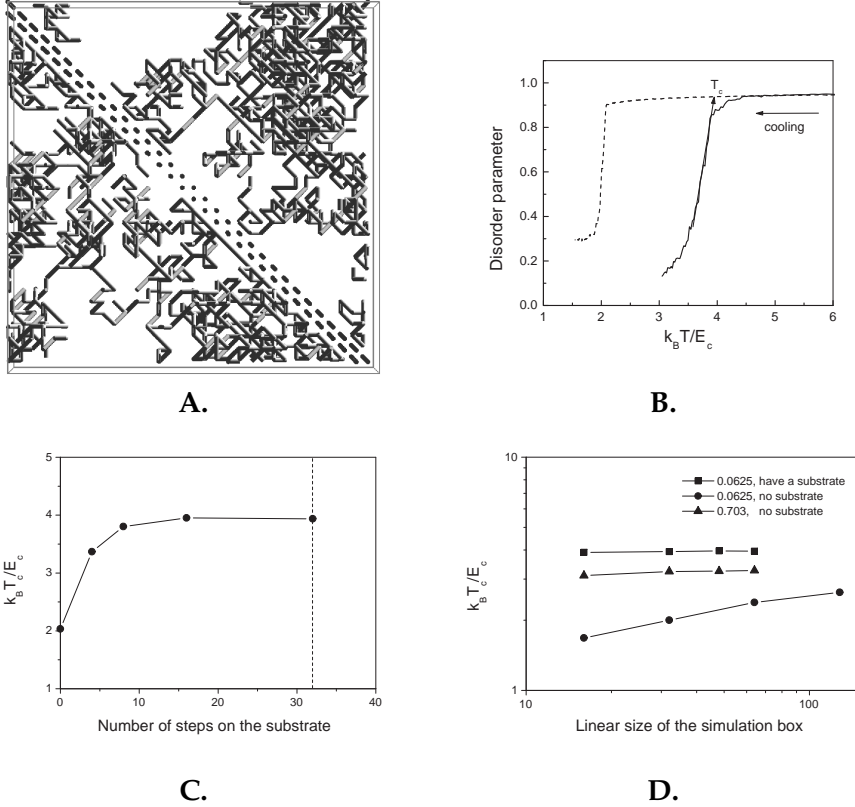


Figure 2: Effect of a terraced substrate on the onset of crystallization upon cooling a sample system with $E_p/E_c = 1$ and $B/E_c = 0$ and with polymer volume fraction 0.0625. (A) Snapshot of an athermal sample system containing one layer of terraced substrate formed by extended chains, which are not included in the polymer volume fraction. Viewing along the extended chains. (B) Disorder-parameter cooling curves for the sample systems with a terraced substrate on a smart cooling (solid line) and under the absence of substrate on a regular cooling (dashed line). The arrow indicates the onset of phase transition. (C) Substrate-size dependence of the onset of crystallization on a smart cooling. (D) Finite-size scaling of the onset of crystallization on cooling for the sample systems with denoted concentrations. All error bars are smaller than the symbols. The segments are drawn as a guide to the eye.

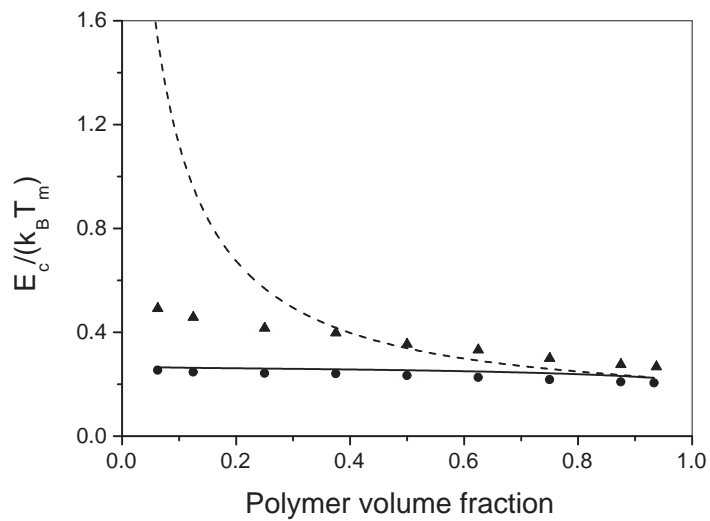


Figure 3: Liquid-solid transition temperatures of the sample system with $E_p/E_c = 1$ and $B/E_c = 0$ vs. polymer volume fractions. The solid spheres are the onsets of crystallization induced by a terraced substrate on a smart cooling, while the solid triangles are the results on a step cooling under the absence of substrate. The error bars are smaller than the symbols. The dashed curve is calculated from Eq. 2, and the solid curve is calculated from Eq. 3.

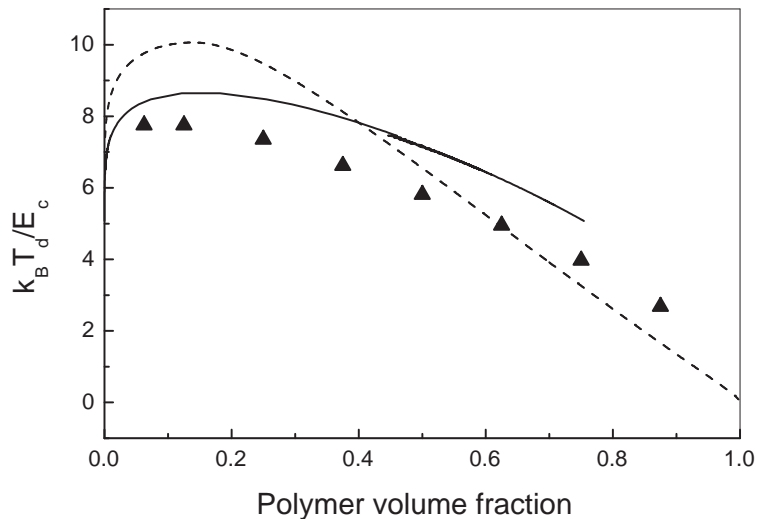
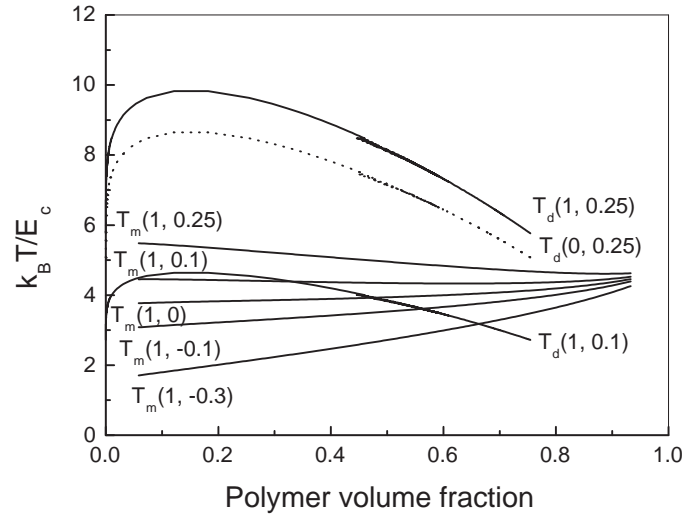
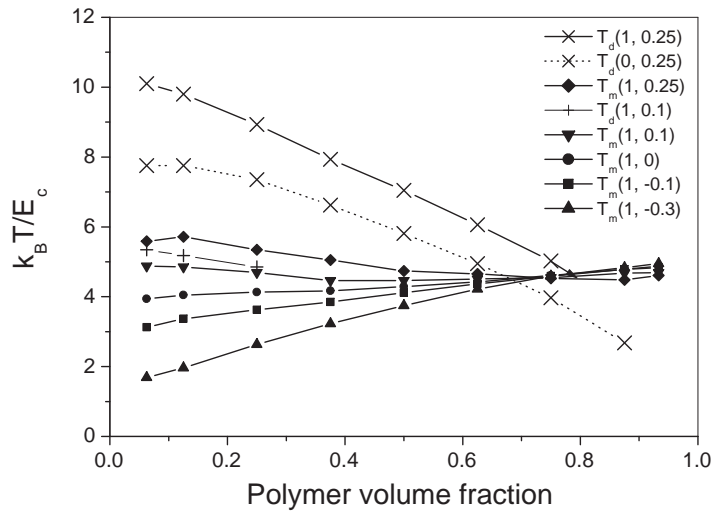


Figure 4: Liquid-liquid coexistence curves (T_d) of the sample system with $E_p/E_c = 0$ and $B/E_c = 0.25$. The solid line is calculated from the classical Flory-Huggins free energy expression for polymer solutions, and the dashed line is calculated from the second-order expansion of the mixing free energy in lattice-cluster theory. The triangles are the onsets of liquid-liquid demixing induced by a terraced substrate on a smart cooling. The error bars are smaller than the symbols.



A.



B.

Figure 5: Liquid-liquid demixing curves (denoted as T_d) and liquid-solid transition curves (denoted as T_m) for the sample system with variable energy parameter settings (denoted as $T(E_p/E_c, B/E_c)$). (A) Theoretical curves calculated from Eq. 3 with $q_{\text{eff}} = q - 2$ (Flory-Huggins approach); (B) Onsets of phase transitions induced by a terraced substrate on a smart cooling. The error bars are smaller than the symbols, and an arrow indicates the monotectic triple point.

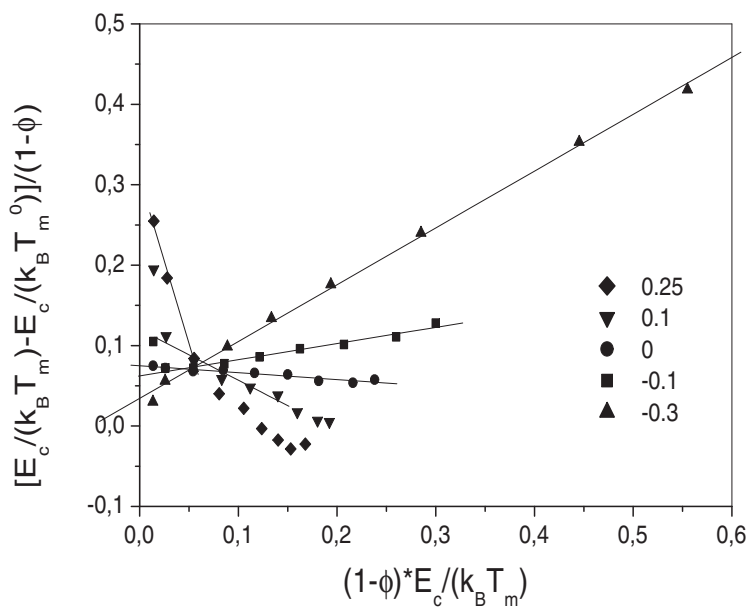


Figure 6: Onsets of crystallization induced by a terraced substrate on a smart cooling in Fig. 5B rescaled according to Eq. 4 with an approximation of $E_c/(k_B T_m^0) = 0.2$. The solid lines are the result of linear regression of the data points without prior liquid-liquid demixing.

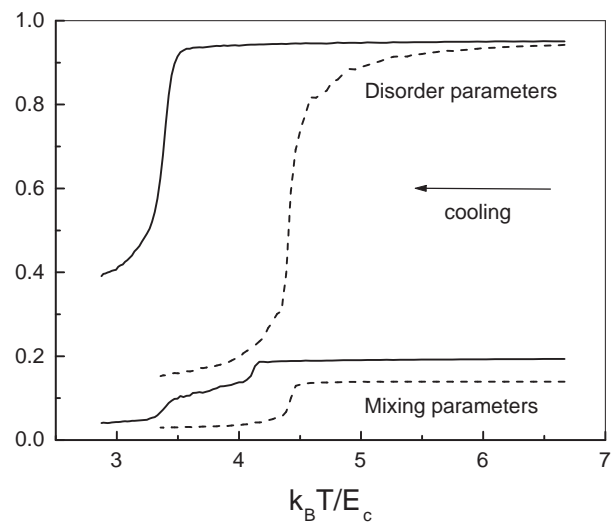


Figure 7: Disorder-parameter and mixing-parameter cooling curves for the sample system with polymer volume fraction 0.8, $E_p/E_c = 1$, and $B/E_c = 0.25$. The solid curves are the results of a regular cooling under the absence of substrate, and the dashed curves are the results of a smart cooling with a terraced substrate.